

Chemical Species Redistribution by Deep Convection and Its Sensitivity to Different Types of Storms

Kaylee Acuff and Mary Barth
National Center for Atmospheric Research
Boulder, Colorado

1. INTRODUCTION

Convective processes within the atmosphere play a large role in the advection of energy, water vapor, and aerosols within the atmosphere. Strong convective storms have the ability to reach great depths where exchange of chemical species and aerosols may occur between the upper troposphere and lower stratosphere. These exchanges potentially have great impacts on the regional and global chemical budgets and radiation balances, as trace species are transported long distances and their atmospheric lifetimes increase significantly. Typically, the distributions of chemical species whose sources are at the surface have high concentrations in the boundary layer and lower concentrations in the free troposphere. However, in the presence of deep convection and strong updrafts, higher concentrations of trace species are transported to the upper troposphere where they reside in the cloud anvil. The fate of the species is then determined by whether or not it is precipitated out of the cloud through wet deposition or transported into the upper troposphere from the cloud outflow region as a gas. Quantifying microphysical and chemical processes within deep convective clouds is essential in determining the chemical species concentrations in the upper atmosphere.

The purpose of this study is to help elucidate the transport of chemical species, both passive and reactive, within two storms that developed in different thermodynamic environments. We contrast the redistribution of carbon monoxide (CO), a passive chemical species, and nitric acid (HNO₃), a highly soluble chemical species, from the two deep convective storms.

The two different storms each occurred near the Colorado-Wyoming-Nebraska border within two days of another. The principle differences in the storms were the environmental conditions in which each evolved and the resulting storm structures. On July 10, 1996, the storm evolved in an unstable environment whose conditions were described by Skamarock et al. (2000). The environment at the time of storm development showed relatively unstable conditions favorable for thunderstorm development and had a CAPE value near 1850 J kg⁻¹ m⁻². The storm that developed on July 12, however, evolved in a less unstable environment with a CAPE value of only 710 J kg⁻¹ m⁻² but with strong shear that reached near 35 m s⁻¹ in the 6 km layer above the terrain. Further details about the environmental conditions that the July 12 storm developed in were described by DeCaria et al. (2000). In both cases, the initial convection developed along the Cheyenne Ridge in southeastern Wyoming as elevated heating and pooling of low-level moisture provided convection initiation.

2. MODEL DESCRIPTION

The storms were simulated using the Weather Research and Forecasting model, WRF, a 3-D, conservative, non-hydrostatic model that is configured to a 160x160x20 km domain with 161 grid points in both horizontal directions and 51 grid points in the vertical direction. A split-explicit time-integration method based on 3rd order Runge-Kutta scheme (Wicker and Skamarock, 2002) is used. Transported scalar quantities predicted by the model are chemical species, water vapor, cloud water, rain, ice, snow, and hail, with hail density $\rho_h = 0.917 \text{ g cm}^{-3}$ and hail intercept parameter for the size distribution $N_o = 4 \times 10^4 \text{ m}^{-4}$. The

microphysics parameterization of Lin et al (1983) is used.

The WRF model is coupled with gas-aqueous chemistry and microphysical transport processes (Barth et al., 2000; 2006). The gas and aqueous chemistry predicts the chemistry of 16 species: O_3 , H_2O_2 , OH , HO_2 , CO , CH_4 , CH_3OO , CH_3OOH , CH_2O , $HCOOH$, NO , NO_2 , HNO_3 , NH_3 , SO_2 , and SO_4^{2-} . The chemical species are each initialized with a single vertical profile. These initial concentration profiles are exactly the same for the two simulations discussed below.

This study focuses on the redistribution of CO and HNO_3 . The CO chemical lifetime (months) is slow compared to the timescale of the convection. CO is a fairly insoluble species and remains in the gas phase during cloud encounters. The HNO_3 chemical lifetime in the gas-phase (~days) is also slow compared to the timescale of convection. However, HNO_3 is highly soluble and is dissolved in the cloud and rain drops where it undergoes microphysical transfer to the ice, snow, and hail. Eventually most of the HNO_3 is rained out.

3. RESULTS

The simulations of the two storms were both initialized with a single (but different) sounding of horizontal winds, potential temperature, and water vapor mixing ratio. Both simulations initiated the convection with the warm bubble method. The July 10 storm was initiated by using 3 diagonally (northwest to southeast) placed $3^\circ C$ warm bubbles (Skamarock et al., 2000), while the July 12 storm was initiated by using two $4^\circ C$ warm bubbles aligned west to east.

Comparisons are made using results after one hour of simulation. At this time in each simulation, both storms display a strong multicell structure. The July 10 storm reflectivity shows three updraft cores (Figure 1) whereas the July 12 storm reflectivity displays four main updraft cores. Both results resemble the observed storm reflectivity. The

July 12 storm reflectivity (Figure 1) has a larger horizontal cloud area, which was 45 km wide and 90 km long, at $z = 9$ km above ground level (agl), while the July 10 cloud area (30 km wide and 75 km long) was significantly less.

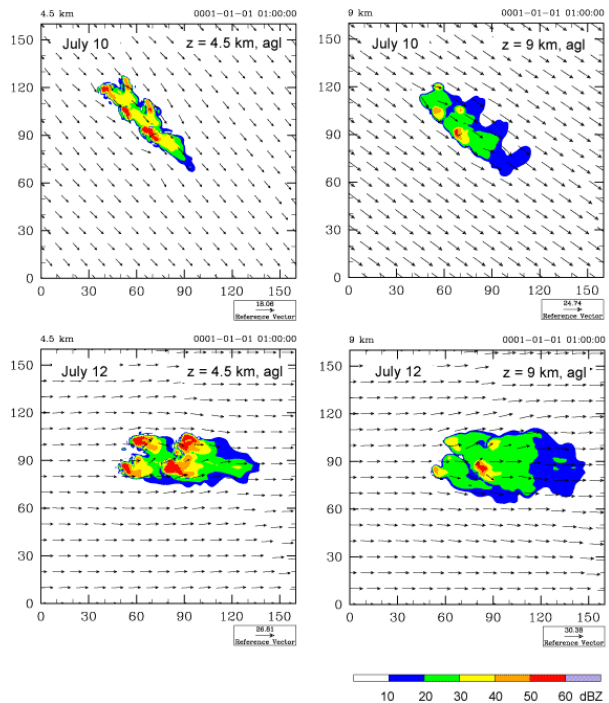


Figure 1. Reflectivity calculated for each storm simulation at $t = 1$ hr, and $z = 4.5$ km, agl (left panels) and at $z = 9$ km, agl (right panels). The top panels are for the July 10 storm and the bottom panels are for the July 12 storm.

Since absorption of chemical species and subsequent reaction in the aqueous phase depends on the existence and magnitude of liquid water, a comparison of the storm hydrometeor fields is examined (Figure 2). The white lines in Figure 2 outline the cloud water field in the vertical cross section at $t = 1$ hr. In this region, the two storms have similar magnitudes of cloud water. However, the July 12 storm has more regions of cloud water because of the four convective cores. The July 12 storm also has a more extensive rain region where aqueous chemistry proceeds. At $z = 10$ km, agl, the July 12 storm shows more total condensate, which is a result of the 4 updraft regions, than the July 10 storm

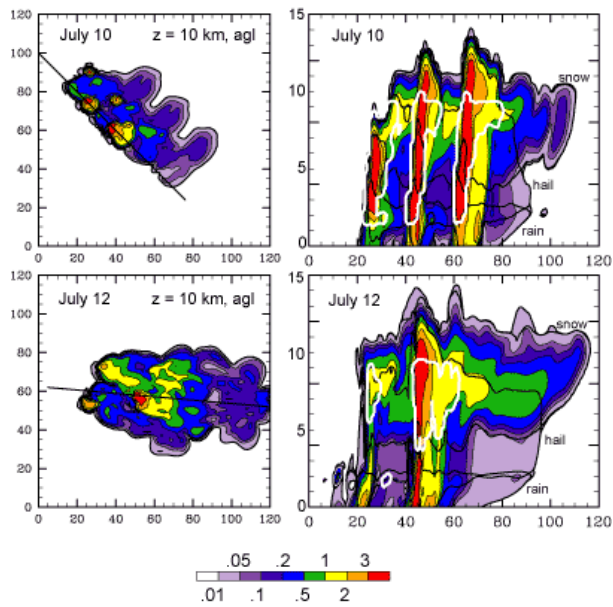


Figure 2. Total condensate mixing ratios (g kg^{-1}) for each simulation at $t = 1$ hr. Left panels are at $z = 10$ km, agl and right panels are vertical cross-sections along the line drawn in the horizontal cross section. White lines in the vertical cross-section denote the cloud water isoline = 0.01 g/kg. Dark, heavy lines are the 0.01 g/kg isoline for snow, hail and rain.

For these short simulation times, CO is an insoluble species (meaning it will remain in the gas phase) and a chemically, passive tracer whose distribution will depend primarily on convective transport. At $t = 1$ hr, higher CO mixing ratios at $z = 10$ km, agl are found in the simulated July 12 storm (recalling that both simulations were initialized the same for the chemical species). Large regions of $\text{CO} > 120$ ppbv are found in the July 12 simulation, while the July 10 simulation has CO mixing ratios between 90 and 120 ppbv in the storm anvil.

HNO_3 is a highly soluble species but has slow chemistry in the gas phase and no aqueous-phase chemistry included in these simulations. Thus, its redistribution by convection will be primarily due to convective transport and dissolution followed by rain out. Total HNO_3 (= gas + cloud water + rain + ice + snow + hail) mixing ratios indicate a substantial loss of HNO_3 near the top of the convective cores and in the anvil region (Figure 4) for both convective storms studied. Because of the abundant cloud water regions

in the July 12 simulation, there is more HNO_3 depletion found in this simulation.

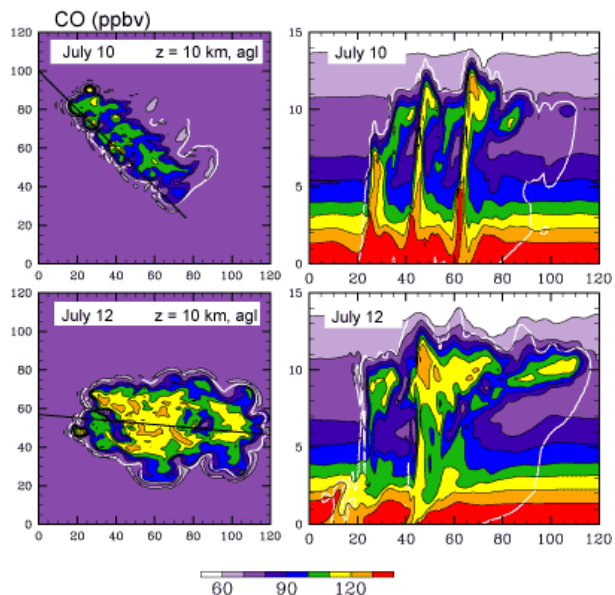


Figure 3. CO (ppbv) mixing ratios for each simulation at $t = 1$ hr. Left panels are at $z = 10$ km, agl and right panels are vertical cross sections along the line drawn in the horizontal cross section. White lines are the total condensate = 0.01 g/kg isoline.

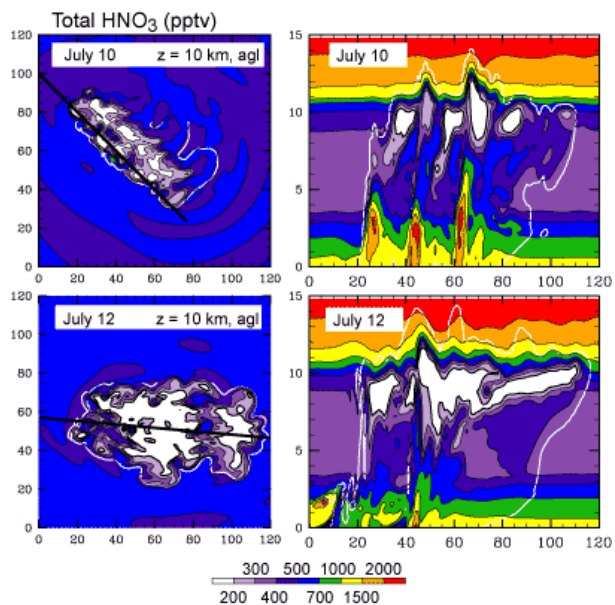


Figure 4. As in Figure 3 but for HNO_3 (pptv) mixing ratios.

By comparing the change in domain-averaged vertical profiles (i.e. average vertical

profile at $t = 1$ hr minus initial vertical profile) between the July 10 and 12 cases, we can examine more quantitatively differences in convective transport of species between these two storms. For CO the change in the domain-averaged vertical profile shows increased mixing ratios at $z = 10$ km, agl. The increase for the July 12 simulation is 3 times greater than that for the July 10 simulation. For HNO_3 the change in the domain-averaged vertical profile shows an increase near the surface for both simulations (due to gas-phase chemistry) and a decrease at $z = 11$ km, agl. The decreased values in the upper troposphere are approximately the same for the two simulations. Thus, the convective processing of HNO_3 (i.e. transport, dissolution, and rain out) for the two multicellular storms is quite similar for this comparison.

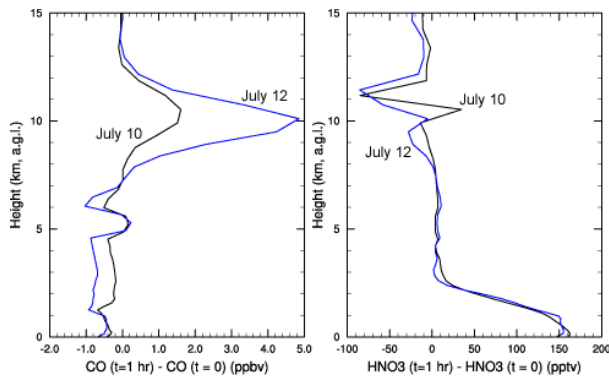


Figure 5. Change in CO (ppbv) vertical profile (left panel) and HNO_3 (pptv) vertical profile (right panel) from $t = 0$ to $t = 1$ hr.

4. CONCLUSIONS

The redistribution of chemical species by two deep convective storms were examined with the WRF model coupled with aqueous chemistry. The thermodynamic environment for the two storms were different in that the July 10 storm had more CAPE ($1850 \text{ J kg}^{-1} \text{ m}^{-2}$) than the July 12 storm (CAPE = $710 \text{ J kg}^{-1} \text{ m}^{-2}$). Model results after 1 hour of integration were compared. These results showed that more CO, a passive, insoluble species, was convectively transported to the upper troposphere in the lower CAPE storm (July 12). This may be a result of the comparison

at an instantaneous time and/or the method of convective initiation which resulted in 3 convective cores for the higher CAPE storm (July 10) and 4 convective cores for the lower CAPE storm at $t = 1$ hour. Differences in HNO_3 were seen in the anvil region where HNO_3 was depleted compared to the background upper troposphere. More HNO_3 was depleted in the low CAPE storm (July 12), but when HNO_3 was averaged over the model domain differences between the two storms were not significant.

To further compare the influence of different types of convective storms on chemical species redistribution, further analysis of these results (i.e., examining a wide range of parameters) will be done. In addition, storm integrated comparisons of the flux of different chemical species to the upper troposphere and to the surface via rain out will be examined.

5. ACKNOWLEDGMENTS

The National Center for Atmospheric Research is operated by the University Corporation for Atmospheric Research under the sponsorship of the National Science Foundation.

6. REFERENCES

- Barth, M. C., W. C. Skamarock, and A. L. Stuart, 2000: The influence of cloud processes on the distribution of chemical species for the 10 July 1996 STERAO/Deep Convection Storm, in International Conference on Clouds and Precipitation Proceedings, Reno, Nevada, USA, 14-18 August 2000, 960-963.
- Barth, M. C., S.-W. Kim, W. C. Skamarock, A. L. Stuart, K. E. Pickering, L. E. Ott, 2006: Simulations of the redistribution of formaldehyde and peroxides in the July 10, 1996 STERAO deep convection storm, to be submitted to *J. Geophys. Res.*
- DeCaria, A.J., et al., 2000: A cloud-scale model study of lightning-generated NO_x in an individual

thunderstorm during STERAO-A, *J. Geophys. Res.*, **105**(D9), 11,601-11,616.

Lin, Y.-L., et al., 1983: Bulk parameterization of the snow field in a cloud model, *J. Clim. Appl. Meteor.*, **22**, 1065-1092.

Skamarock, W. C., et al., 2000: Numerical simulations of the 10 July STERAO/Deep Convection Experiment convective system: Dynamics and transport, *J. Geophys. Res.*, **106**, 19,973-19,990.

Wicker, L. J., and W. C. Skamarock, 2002: Time Splitting Methods for Elastic Models Using Forward Time Schemes. *Mon. Wea. Rev.*, **130**, 2088-2097.